Heliyon 10 (2024) e37509

Contents lists available at ScienceDirect

Heliyon

journal homepage: www.cell.com/heliyon

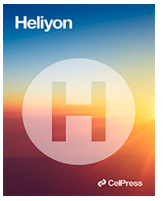

Research article

The incident photons cut-off energy, the optical linear equations and the electron phonon interactions in ZnO thin films annealed at different temperatures

Vali Dalouji

Department of Physics, Faculty of science, Malayer University, Malayer, Iran

ARTICLE INFO

Keywords:
The ZnO thin films
The post
Annealing temperature
The optical linear equations
Skin depth
Steepness parameters
Electron phonon interaction

ABSTRACT

The using RF-magnetron sputtering, the ZnO thin films were deposited on glass substrates at room temperature. Then using an electrical furnace in the presence of argon gas, they were annealed at different temperatures (400–600 °C). It was found that with taking $N_c = 4$, $Z_a = 2$, $N_e = 8$ for ZnO films for covalently bonded crystalline and amorphous chalcogenides, the constant β has values of about 0.37 ± 0.04 and for halides and most oxides that have ionic structure the constant β has values of about 0.26 ± 0.04 eV. It can be seen that with increasing annealing temperature absorption edge these films have a shifting behavior towards larger wavelength. Due to shifting behavior of defects distribution of atoms into films, the values of the cut-off energy, E cut-off and the λ cut-off of these films were about 3.48 eV and 355 nm, respectively. The ZnO films annealed at 500 °C specially above 3 eV have maximum value of optical density. The different linears fitting of ln (α) for films were obtained as y = Ex + F where 10<E < 12.5 and 14<F < 16. The ZnO films annealed at 600 °C have minimum value of electron phonon interaction ($E_{e\text{-}p}$) in a bout of 0.858 eV. The optical band gap and disordering energy plots of these films can be fitted by linear relationship E_U and E_g = 0.0989–0.148 E_U. We found that as deposited ZnO films have minimum value of steepness parameter σ in about of 30.93 × $10^{-2}eV$.

1. Introduction

Semiconductor materials with nonlinear optical properties are of great importance. These materials alter the optical properties of the light during its propagation. So, these materials can be used in different applications such as optical information storage, optical switching, optical communication networks, and signal processing, optical waveguides [1]. Nonlinear optical properties of the metals oxides thin films have a great attraction now a day. For example, the metals oxides thin films such as the ZnO thin films have promising optoelectronic applications due to its good third order nonlinear generation [2,3]. Because of its unique opto-electronic properties, chemical and thermal stability, low cost, and biological activity ZnO has become an alternative to TiO_2 in photocatalytic reactions. The ZnO also is an n-type semiconductor with wide bandgap energy of 3.37 eV and large exciting binding energy of 60 meV at room temperature which slowdowns the recombination of electron-hole pair. In addition, ZnO possesses higher quantum efficiency, allowing the absorption of larger fractions of UV region and visible region than to TiO_2. Physical methods include sputtering techniques, pulsed laser deposition, and molecular beam epitaxy (MBE) were used for deposition of ZnO thin films [4–12]. The ZnO thin films can also be prepared via chemical methods, such as chemical bath deposition [13], chemical vapor deposition [14], atomic layer

E-mail address: dalouji@yahoo.com.

https://doi.org/10.1016/j.heliyon.2024.e37509
Received 22 June 2024; Received in revised form 9 August 2024; Accepted 4 September 2024
Available online 7 September 2024

deposition, spray pyrolysis, printing, sol–gel spin coating, and electrochemical deposition, which are simpler methods and generally less costly. The control of the ZnO nano particles stability, solubility, and surface structure, shape and aggregation properties represents some of the key roles for ZnO nano particles industrial and other practical applications [15–17].

One of the most prominent characteristics and indicators of interest to many scientists in the present era who work on material science and their properties and applications is the responses of these materials to external photon radiation on them with different wavelengths. The type of these responses, which can be linear or non-linear of different orders, can be very useful in designing and manufacturing different optical and electrical components.

The results obtained from the research of other scientists show that the ZnO thin films are predicted to have non-linear responses in the radiation of different photons with different wavelengths, but of the third order, and this result is very useful and productive for these materials.

In this new work, firstly, we were able to model this nonlinear response as simulated mathematical equations by using mathematical modeling, and we were able to model a specific mathematical equation for each annealed sample at each temperature. Different equations that were modeled for different samples were related by different numerical constants. After modeling the equations for different samples, some of the results and optical data of these samples were measured, which were interesting examples of the non-linear response of these materials to radiation photons with different wavelengths.

In this article, as practical examples, we examined different values of the optical density and the depth of the ZnO thin films shell, that is, the distance from the inside of the material to its surface where the intensity of incident photons reaches $1/e$ of their intensity on the surface of the ZnO thin films [17]. The study of different electron-photon interaction values measured at different wavelengths was another example of non-linear responses of ZnO thin films, which showed different values at different annealing temperatures. Then, by studying the transmission spectra in ZnO thin films, the isolated single oscillator model was used in the normal dispersion region, and different values of the refractive index of the ZnO thin films were obtained, which was a function of the wavelength of the incident photons. These obtained results, were in good agreement with the other results obtained for these optical constants.

In the following, then the relationship between all these optical results obtained with mathematical modeled equations was investigated and we were able to use this mathematical model to compare the different values of the optical gap with the different values of the Urbach energy, which actually indicates the degree of irregularity of the material.

At the end, the relationship between all these optical results with the physical characteristics of the ZnO thin films, such as the surface roughness of the ZnO thin films, the size of the nanoparticles, as well as the values of the annealing temperature, were investigated, and the non-linear responses of these optical results were proved in many cases in the ZnO thin films.

As a result, therefore, the aim of the present paper is focusing on complement the estimation, investigation and study some other

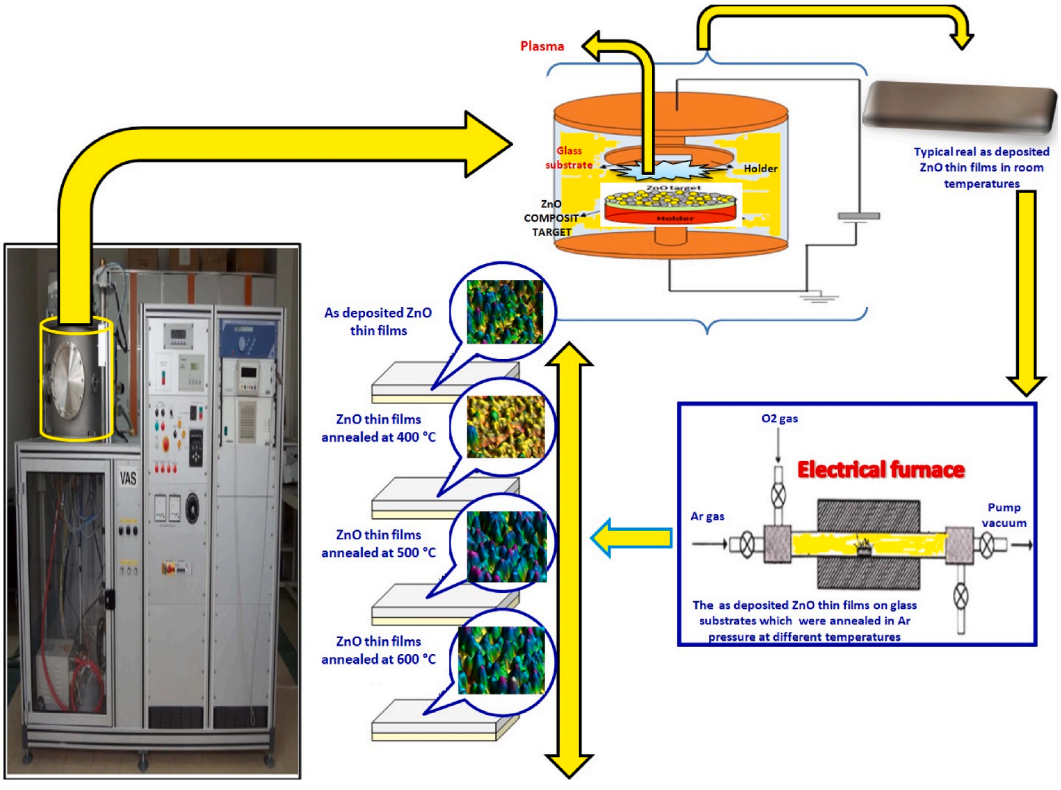

Fig. 1. Schematic of depositions processing using real RF – MAGNETRON VAS – SPUTTERING SYSTEM and typical real as deposited ZnO thin films deposited at room temperature then they were annealed at different temperatures 400, 500 and 600 °C in Ar atmosphere pleasure.

optical and topographical properties of ZnO thin films. In the previous works [18–20], some optical properties of these films were studied however Here, we have investigated the nonlinear behavior of some parameters that we have not studied before. we investigated many properties of this new processing of ZnO thin films, in there we want to investigate some nonlinear optical properties of these materials by using linear mathematical equations, and by obtaining some new optical parameters of these films and their relationship with their surface quality, let's implement a mathematical simulation model with these non-linear optical properties. The main purpose of this manuscript is to be to study the steepness parameter (σ), electron-phonon interaction ($E_{e\text{-}ph}$), optical density (D_{opt}), coordination number constant (β), skin depth (δ) and linear optical equations on the ZnO thin films deposited at room temperature and ZnO thin films annealed at different annealing temperatures 400, 500 in electrical furnace with Ar flux for 60 min.

2. Experimental details

The ZnO thin films were prepared on glass substrates by VAS- system rf magnetron system with a 13.56 MHz power supply and ZnO composite target (100 mm diameter and 5 mm thickness with high purity (99.99 %)) in room temperature (Fig. 1). The reactor consisted of two electrodes with different sizes. The smaller electrode was ZnO composite target as powered electrodes in the first and the second steps of deposition respectively and the other electrode was grounded substrates. The distance between the powered electrode and the substrate was maintained at 60 mm. The chamber was evacuated to a base pressure of about 7×10^{-5} mbar prior to the deposition and then the pressure was raised to the desired ambient pressure using Ar and O_2 gas flow which it causes to be reach work pressure of about 7×10^{-2} mbar. Before using the glass slides as substrates at room temperature in a vacuum chamber, they were thoroughly washed and completely cleaned in an ultrasonic device for 20 min containing distilled water and ethanol in a ratio of 2:1. Then we washed them again with acetone and put them in the appropriate places of the substrate in the sputtering system.

Then, these ZnO thin films at different annealing temperatures of 400, 500, and 600 °C were annealed in electrical furnace with Ar flux for 60 min.

The thickness of the films was measured using a Tencor Alpha-step 500 profiler. The scanning electron microscope (SEM) (VEGA-TESCAN LMU) was used to estimate nanoparticle size, the characterizations and the surface morphology of the films. AFM (Veeco Instruments, Inc., USA) in the non-contact mode was used to obtain the surface topography of the ZnO thin films, average particle size and root mean square (RMS) roughness. The Atomic Force Microscopy (AFM) with standard tipped CSC12 cantilever of 0.03 N/m nominal stiffness in contact mode over a scan area of 2.2 μm × 2.2 μm.

The optical properties were performed using a double-beam UV–Vis spectrometer in the range of 300–800 nm. The transmittance and reflectance measurements of films were performed by Varian Cary-500 spectrophotometer in the range of 200–2500 nm (Varian Inc, CA, USA).

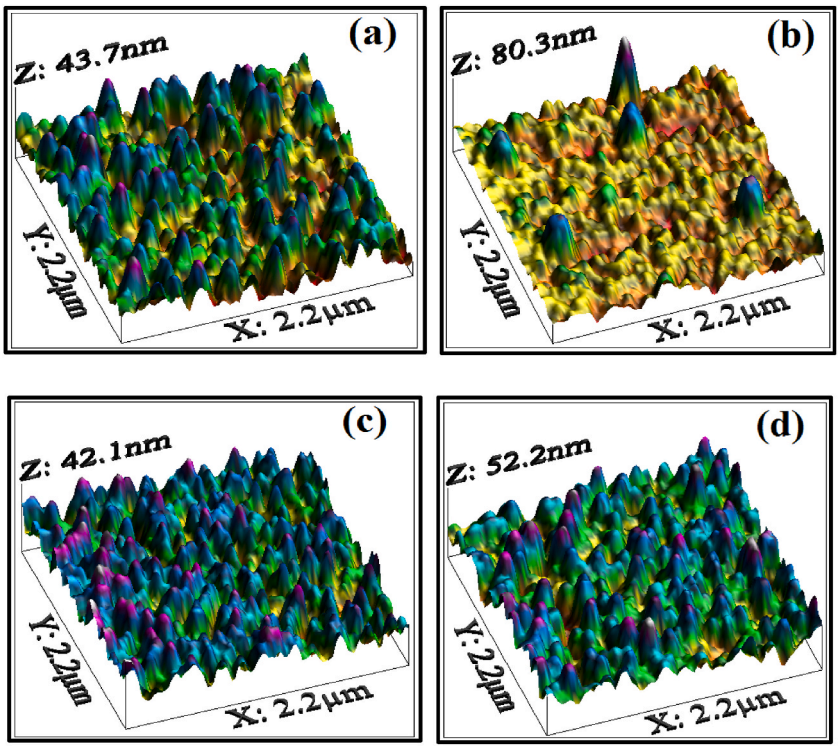

Fig. 2. The 3D AFM images (2.2 × 2.2 μm^2) of ZnO films (a) as deposited ZnO films and ZnO films annealed at (b) 400, (c) 500 and (d) 600 °C.

3. Results and discussions

3.1. AFM images analysis

The AFM images in surface area section, 2.2 × 2.2 μm^2, of films were shows in Fig. 2(a–d). The RMS roughness of as deposited ZnO films and ZnO films annealed at 400, 500, 600 °C were in about 7.238, 8, 7.056 and 7.817 nm, respectively. According to these AFM images of films and RMS data obtained from WsXM software and AFM images file data, the distributions of nano particles on ZnO films surfaces can be analyzed by variations of annealing temperature values. The RMS roughness of these films was changed in the range of 7–8 nm with variations of annealing temperature, and we found that the lowest value of surface roughness was occurred in films annealed at 500 °C. In fact, annealing temperature of films at 500 °C in an argon medium was a critical temperature for oxidative

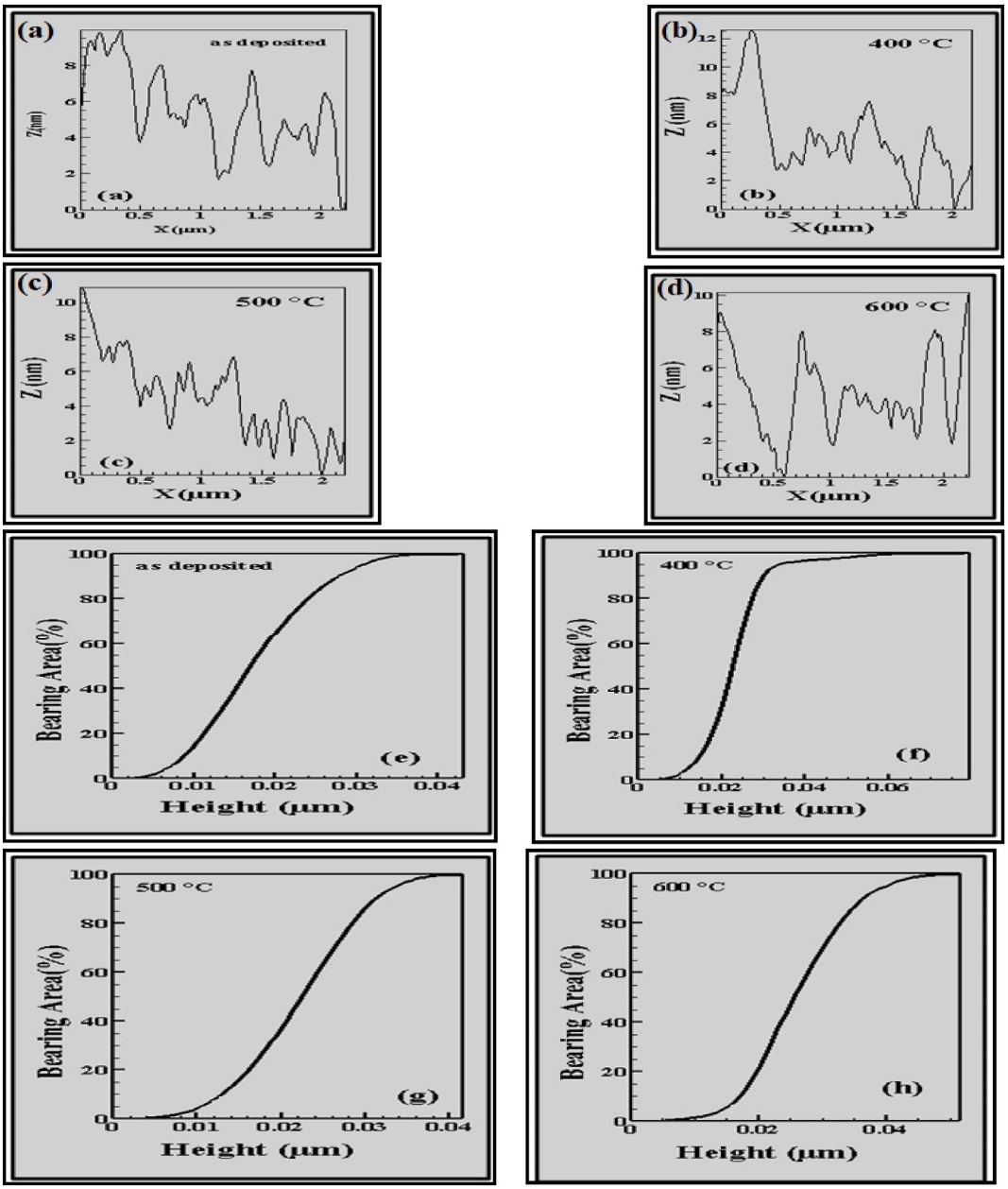

Fig. 3. Variations of the Z (nm) values of films versus the X (μm) values obtained from AFM files data by WSxM software for (a) as deposited ZnO films, ZnO films annealed at (b) 400, (c) 500 and (d) 600 °C, and variations of the bearing area values of films versus the values of the mean height (μm) nanoparticles on films surfaces obtained from AFM files data for (e) as deposited ZnO films, ZnO films annealed at (f) 400, (g) 500 and (h) 600 °C.

structure changes. The values of nano particles size of films surface were increased from 20 to 30 nm, due to the increasing energy and hence the increasing in surface mobility due to the increasing in the annealing temperature. The increased kinetic energy, high energy heat and high surface mobility were principal factors that were increased the surface dispersion of films. Also, these factors were formed a structure with larger grain size in all films. On the other hand, as the annealing temperature were increased, the particle size distribution was changed and it do not change much their particle sizes and total variations remains in total films. Because sputtering, which is a completely random process, this entire process is a combined process, and both metallic and non-metallic nanoparticles are sputtered, and considering that the rate of accumulation of metals is higher than that of non-metals, it is expected that the rate of accumulation of zinc nanoparticles is higher than that of oxygen nanoparticles. Because the substrates in this zinc oxide films production experiment were kept at room temperature, so as soon as the nanoparticles sit on the substrates, their mobility quickly moves to low energy values, and after the nanoparticles land on the substrates. They do not have much time the opportunity to find a point on the substrate that has the lowest level of potential energy (relative to a fixed source such as the surface of the substrate), so they come to rest at the first point where they lose their mobility. When the sputtering time was increased and more and more particles hit the surface of the substrate and the thickness of the layer was increased, it is naturally expected that the temperature of the substrate will increase by a small amount. The temperature of the substrate decreases respect to the upper nanoparticles. In these new conditions, particles and nanoparticles landing on the substrate, after the formation of grains, have an initial mobility, which according to the new existing conditions, now nanoparticles have more opportunity to move on the surface of the substrate and points on the surface that have an energy level find a lower level and reach equilibrium there and lose all of its energy and its mobility reaches zero at this moment. Annealing of the films after depositions them by sputtering system, by an electric furnace, can also create similar conditions on the arrangement and redistribution of nanoparticles on the substrates. This redistribution of nanoparticles may even be the optimal conditions for changing the network structure and in certain cases it can also be effective in crystal growth.

When the ZnO films were annealed at 400 °C, this high temperature forced the nanoparticles to move on the layers. In this situation, the mobility of the particles was increased and forced them to move with the opportunity that the nanoparticles found, some of them, which were placed in inappropriate places, tried to reach the points with the lowest potential energy level, but due to the sudden increase in energy the mobility of nanoparticles, they collided with other nanoparticles on their way and created larger particles and reached their saturation state.

This will increase the size of the particles and also increase the roughness of the layer surface. The data obtained from the AFM images show that the surface roughness of films annealed at 400 °C is equal to 8 nm, which is rougher than the layers deposited at room temperature, which have RMS roughness of about 7.2 nm.

By increasing the annealing temperature to 500 °C, these saturated nanoparticles now tend to move some of them to the points of the surface that have lower potential surface energy, and this reduces the roughness of these layers. The data obtained from AFM images shows that the surface roughness of films annealed at 500 °C is equal to about 7 nm, which were smoother than the films annealed at 400 °C, which have RMS roughness of about 8 nm.

By increasing annealing temperature to 600 °C, also due to the sudden increase in the mobility energy of the nanoparticles, they collided with other nanoparticles on their way and created larger particles and reached their saturation state. In this situation, it is expected that the surface roughness of the layers will increase, the results obtained from the pictures AFM images that the surface roughness of the films annealed at 600 °C is equal to 7.8 nm compared to the films annealed at 400 °C which have the roughness is about 7 nm, they were rougher.

Fig. 3(a–d) show the variations of the Z (nm) values versus the X (μm) values obtained from WSxM software and using AFM files

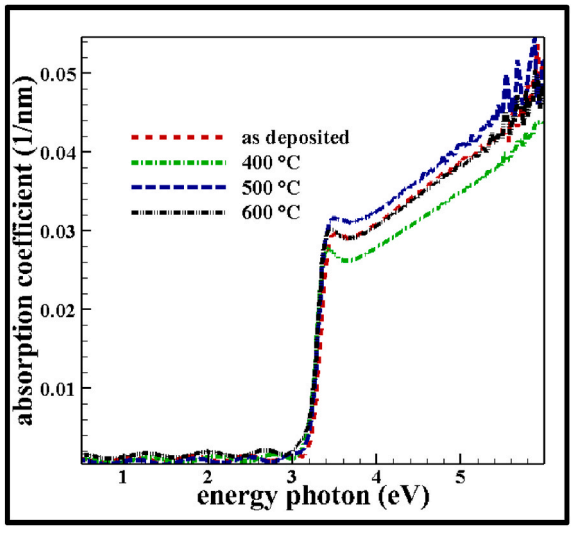

Fig. 4. Variations of the optical absorption coefficients α versus energy photon (eV), for as deposited ZnO films and ZnO films annealed at 400, 500 and 600 °C.

data for as deposited ZnO films and ZnO films annealed at 400, 500 and 600 °C, respectively. The surface scanned of the films by the atomic force microscope (AFM) tip was about 2.2 × 2.2 μm^2, in this surface scanned, the maximum numerical value for the value of x -axis was to be 2.2 μm. Variations of the height particles value on this the scanned surface were indicated that the ZnO films annealed at 400 °C has a sharp variation in about 12 nm and it indicated that the films can be have a phase changing. The ZnO films has fewer ups and downs at room temperature and the peaks have a gentle slope than other temperatures. In terms of structure, the graphs are close to each other. Fig. 3(e–h) shows variations of the bearing area (%) values of films obtained from WSxM software versus the values of the mean height (μm) nanoparticles on films surfaces for as deposited ZnO films and ZnO films annealed at 400, 500 and 600 °C, respectively. In fact, these values obtained were indicated that there was the amount of vacuum, zero coverage (cavity) and monolayer and insulation. These results also shown that very low zero coverage value was occurred in the ZnO films annealed at 500 and 600 °C which their monolayer was very high in about 95 %, however in as deposited ZnO films the zero coverage was about 5 and they were obtained very high monolayer which it was more than 100 %.

3.2. Optical studies

3.2.1. Optical coefficients

Fig. 4 shows the variations of absorption coefficients values versus photon energy for as deposited ZnO films and ZnO films annealed at 400, 500 and 600 °C. So, the absorption coefficients of ZnO thin film can be calculated using spectroscopy spectra, the following relation [21].

$$\alpha = \frac{1}{d}\ln\frac{(1-R^2)}{2T} + \left(\frac{(1-R)^4}{4T^2} + R^2\right)^{1/2} \quad (1)$$

The spectral transmission T and the spectral reflection R were measured at normal incidence in the wavelength range 200–2500 nm. With the increasing of energy from 3.1 to 3.2 (eV), the optical absorption coefficient of the ZnO films was also increased sharply, because in this energy range the frequency of the electromagnetic wave is close to or equal to the frequency of the resonant electrons into the ZnO films molecules. Also, with increasing annealing temperature, the values of absorption edge were obtained a shift of towards larger wavelengths. This shifting absorption edge of ZnO films towards larger wavelengths can be due to the variations of size of nanoparticles in to these films. In the absorption spectra of ZnO films, an exaction peak in about 385 nm was observed which changing of its intensity with a changing in the annealing temperature values was in consistent in the nanoparticles size. Also, a small variation in the crystal structure after annealing temperature due to this changing were occurred. That is, the nanoparticles size to be become larger than with increasing of values of annealing temperature and the amount of exaction energy also in these films was increased [22].

3.2.2. Optical density

Fig. 5 shows the variation of the optical density with the photon energy for as deposited ZnO films and ZnO films annealed at 400, 500 and 600 °C investigated in this study. The optical density was calculated using the following relation [23]:

$$\text{Optical density} = \alpha d \quad (2)$$

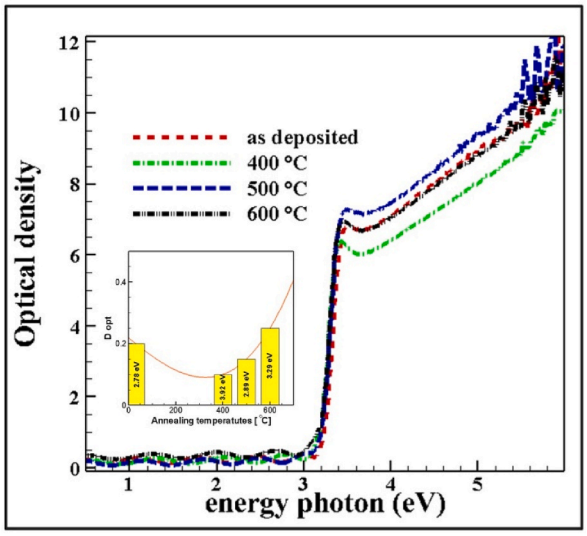

Fig. 5. The variations of optical density D_{opt} of as deposited ZnO films and ZnO films annealed at 400, 500 and 600 °C, versus photon energy (eV). Inset: Variations of D_{opt} and the optical gap of films versus annealing temperatures.

Where d is the thickness of the films, the thickness is fixed (230 ± 5). Fig. 5 shows the values of optical density for as deposited ZnO films and ZnO films annealed at 400, 500 and 600 °C. The values of optical density were to be typically in the range 0.5–6 eV. The behavior of optical density diagram similar to the behavior of optical absorption coefficient diagram of films. The optical density for all the films were to be constant between 1 and 3eV, which they were increased with a steep gradient after 3 eV.

3.2.3. The skin depth

The skin depth δ of films is the value of thickness which the optical photon intensity turns out to equal ($1/e$) of its value on the surface of the films. The value of δ depends on two parameters, the photon frequency and the value of films conductivity, then its values were inversely proportional to both. Therefore, the optical band-gap energy will strongly can be depend on these parameters, high the skin depth was resulted low the narrower band gap and vice versa [24,25]. The skin depth $\boldsymbol{\delta}$ for as deposited ZnO films and ZnO films annealed at 400, 500 and 600 °C have been evaluated via the below relation [26]:

$$\boldsymbol{\delta = 1/\alpha} \tag{3}$$

Where α is the optical absorption coefficients. The variations of the skin depth of the as deposited ZnO films and ZnO films annealed at 400, 500 and 600 °C with the photon energy were displayed in Fig. 6. It was found that with increasing of the photon energy, the skin depth of films was decreased until it arrived at the cut-off wavelength. The value of the incident photons cut-off energy, $E_{cut\text{-}off}$, of the films was about 3.48 eV and the value of the $\lambda_{cut\text{-}off}$ was about 355 nm. The highest skin depth values were occurred for the ZnO films annealed at 500 °C. Because the films annealed at 500 °C have the lowest RMS roughness value of about 7 nm, so when the photons land on the surface of these films, their scattering is greatly was reduced compared to other films. This factor was caused that the intensity of the photons entering these films was increased compared to other films, and more photons enter these films than other films.

Naturally, it was expected that when a large volume of photons entered in to the films annealed at 500 °C compared to other films, their penetration into these films will increase and the depth of the shell will increase accordingly. Therefore, the intensity of the incident photons into these films was directly related to the penetration rate of the photons into these films and hence it has a direct relationship to the depth of the shell.

3.2.4. Optical energy gap determination

The real and imaginary parts of the dielectric constants of films were determined by the following equations [27]:

$$\boldsymbol{\varepsilon_1 = n^2 - k^2 = \varepsilon_\infty - \left(e^2 N / 4\pi^2 c^2 \varepsilon_0 m^*\right) \lambda^2} \tag{4}$$

$$\boldsymbol{\varepsilon_2 = 2nk = \left(\varepsilon_0 w_p / 8\pi^2 c^3 \tau\right) \lambda^3} \tag{5}$$

Where ω_p is the plasma frequency, ε_∞ is the high frequency dielectric constant, e is the electronic charge, N is the free carrier concentration, m^* is the effective mass of free carrier, s is the optical relaxation time, and c is the velocity of light. The variations of real and imaginary parts of the dielectric constant of films versus photon energy (eV) were shows in Fig. 7. The values of real part of the dielectric constant were increased with increasing photon energy. It can be seen that the optical band gaps of films were obtained from the intersection of the real part of the dielectric constant of films and imaginary parts of the dielectric constant of films versus photon

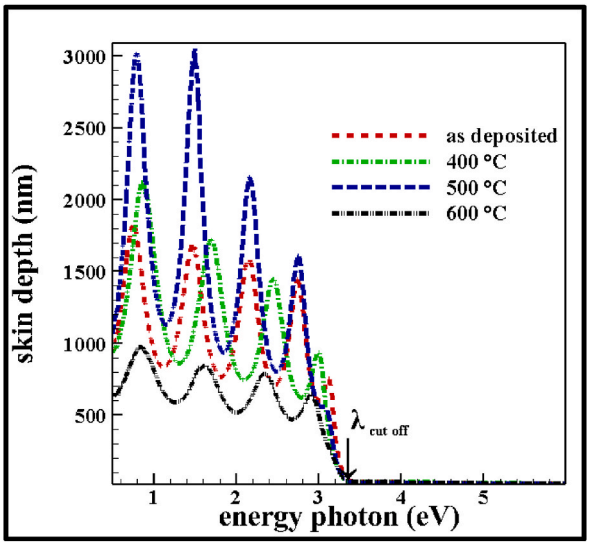

Fig. 6. The variations of the skin depth (nm) of as deposited ZnO films and ZnO films annealed at 400, 500 and 600 °C versus photon energy (eV).

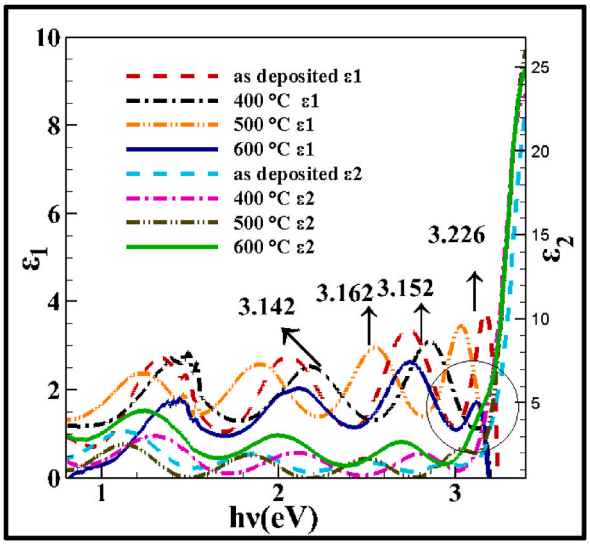

Fig. 7. Dependences of the real and imaginary parts of the complex dielectric constants for as deposited ZnO films and ZnO films annealed at 400, 500 and 600 °C with energy photon (eV).

energy (eV). The optical energy band gap was 3.226, 3.152, 3.162 and 3.142 eV for as deposited ZnO films and ZnO films annealed at 400, 500 and 600 °C, respectively. It can be seen that the optical energy band gap values by increasing annealing temperature have a oscillates behavior. These results observed may also be due to correlated with the distribution defects of atoms. The magnitude of the optical energy band gap values differs within the range of 3.1 eV and 3.3eV.

3.2.5. Absorption band tail (Urbach energy)

Phonons, impurities, exactions, and structural disorders in the materials have been associated with the observed exponential tails [28–31]. The optical absorption spectra of these films were taken in the ranges of 200–2500 nm. The optical band gap energy of films was determined using the following equation [32].

$$\alpha h\nu = \mathrm{A}\ (h\nu - \mathrm{E_{opt}})^{\mathrm{n}} \tag{6}$$

Where α is the absorption coefficient, $h\nu$ is the incident photon energy, A is a constant and E_{opt} is the optical band gap. Values of n are 2 and 1/2 for direct and indirect transitions, respectively. These values in consistent with amorphous or glassy materials for a band tailing in the forbidden energy band gap. The band tailing might be due to from random fluctuations of the internal disorder in to films. So, from obtained above results, the Urbach relation for these films shows as follows [33].

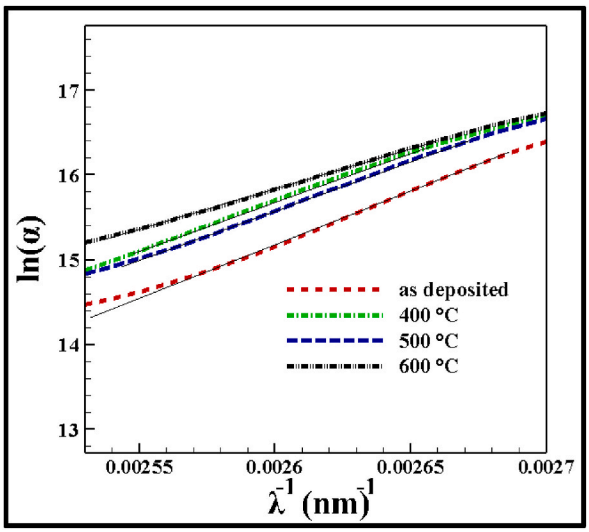

Fig. 8. Dependences of variations of ln (α) for as deposited ZnO films and ZnO films annealed at 400, 500 and 600 °C upon the $\lambda^{-1}(\mathrm{nm})^{-1}$.

$$\alpha\ (\mathbf{v}) = \mathbf{B}\ \exp\ (h\nu/\Delta \mathbf{E}) \tag{7}$$

Where B is a constant and $\Delta E = E_u$ is the width of the band tail of the electron states. From Fig. 8, Urbach energy, E_u of films was determined from the slope of plot ln(α) versus λ^{-1} $(nm)^{-1}$. The calculated values of the band tail energy E_u and the constant α_0 were record in Table 1. The empirical equations from linear fitting ln (α) for different films that is; as deposited ZnO films and ZnO films annealed at 400, 500 and 600 °C, upon the $\lambda^{-1}(nm)^{-1}$ were record in Table 2.

Regarding the obtained results, several linear relationships can be defined between the optical band gap energy and the Urbach energy of as deposited ZnO films and ZnO films annealed at 400, 500 and 600 °C shown in Fig. 9(a and b). Extracting an experimental equation form the linear fitting of the data as presented in equation (8), a notable decreasing in the optical band gap energy along with a gradual increasing in the Urbach energy of as deposited ZnO films and ZnO films annealed at 400, 500 and 600 °C can be highlighted. To get the relations between E_g and E_U, as shows in Fig. 9(a and b), the plots of the values can be fitted. It can be observed that the interrelation between E_g and E_U has a linear relationship. The empirical equation from these linear fitting was given as

$$\mathbf{E_g} = \mathbf{0.0989 – 0.148\ E_U} \tag{8}$$

The average value of the constant α_0 of relation (7), which also can be obtained from the linear fitting model presented of Fig. 9 (c) were to be equal to 0.989 eV, which represents the band gap energy in the case of the absence of tailing. The linear relation between band gap energy and the width of the Urbach tail was resulted for other semiconductors [33–35].

The Urbach energy was defined as $E_U = k_B T/\sigma(T)$, which indicates as the width of the exponential tail in the absorption spectra at temperature T. The value of absorption coefficients of the films below the free exaction peak were obtained using the Urbach's rule [36].

$$\alpha = \boldsymbol{\beta}\ \mathbf{exp}\ [\ \boldsymbol{\sigma}(\mathbf{T})\ (\mathbf{E} - \mathbf{E_0})\ /\mathbf{k_B T}] \tag{9}$$

Where α is the absorption coefficient as a function of photon energy, E_0 and β are the characteristic parameters of the materials, $\sigma(T)$ is the steepness parameter, and k_B is the Boltzmann constant. We rewrite equation (9) as

$$\ln\ (\alpha) = \mathrm{Ln}\ (\beta) + [\sigma(T)\ (E\ /k_B T) - \sigma(T)\ (E_0\ /k_B T)] \tag{10}$$

If a comparison between Equations (7) and (10) was held, one can deduce that

$$(\boldsymbol{\beta}) + \boldsymbol{\sigma}(\mathbf{T})\ (\mathbf{E}\ /\ \mathbf{k_B T}\ )\ ;\ \mathbf{E}\ /\mathbf{E_u} = \boldsymbol{\sigma}(\mathbf{T})\ /\ \mathbf{k_B T} \tag{11}$$

The temperature dependence of the steepness parameter of as deposited ZnO films and ZnO films annealed at 400, 500 and 600 °C were shown in Fig. 10 (a) and the steepness parameter at each temperature has been extracted by fitting the absorption data to equation, $\mathbf{E_U = k_B T/\sigma\ (T)}$.

Furthermore, steepness parameter of ZnO films also were determined the strength of electron-phonon interactions and both were related to each other following relationship [36]:

$$\mathbf{E_{e\text{-}p} = 2/\ 3\sigma} \tag{12}$$

Fig. 10 (b) shows the variations of steepness parameter and electron - phone interaction of as deposited ZnO films and ZnO films annealed at different temperatures of 400, 500 and 600 °C. It was demonstrated that the values of steepness parameters were an increasing function with annealing temperature while electron-phonon interaction were an decreasing function with annealing temperature.

3.3. Determination of the optical and electrical conductivity

To studding relation between electronic and optical responses of ZnO films under variations of annealing temperature, we resulted that the value of real part of optical conductivity (σ_{op}) from the imaginary dielectric constant ε_2 and optical frequency ω, where $\sigma_{op} =$

Table 1
The values of the direct band gap energy (E_g), the band tail width (E_U), steepness parameter (σ) and electron phonon interaction ($E_{e\text{-}p}$) and RMS of as deposited ZnO films and ZnO films annealed at 400, 500 and 600 °C.

Sample no.	Wavelength of absorption edge (nm)	EU (eV)	Eg (eV)	The constant α0 (1/nm)	Steepness parameter σ (× 10^{-2}eV)	Electron phonon interaction Ee-p (eV)	RMS (nm)
ad deposited ZnO films							
ZnO films annealed at 400 °C	386.385	0.0824	3.226	0.394	30.93	2.15	7.23
ZnO films annealed at 500 °C	387.633	0.0912	3.152	0.404	63.49	1.05	7.99
ZnO films annealed at 600 °C	388.804	0.0898	3.162	0.433	74.16	0.89	7.05
	388.927	0.0966	0.413	0.413	77.85	0.85	7.81

Table 2
The empirical equations from liners fitting ln (α) of as deposited ZnO films and ZnO films annealed at 400, 500 and 600 °C, upon the $\lambda^{-1}(nm)^{-1}$ and the single-oscillator energy and dispersions energy parameter, constant β.

Sample no.	Mathematical - optical line equations	E0 (eV)	Ed (eV)	The constant β
ad deposited ZnO films				
ZnO films annealed at 400 °C	y = 12.13x + 14.48	5.28	14	0.22
ZnO films annealed at 500 °C	y = 10.93x + 14.88	4.89	22.4	0.35
ZnO films annealed at 600 °C	y = 11.13x + 14.84	6.98	62.2	0.97
	y = 10.35x + 15.20	6.01	50.3	0.78

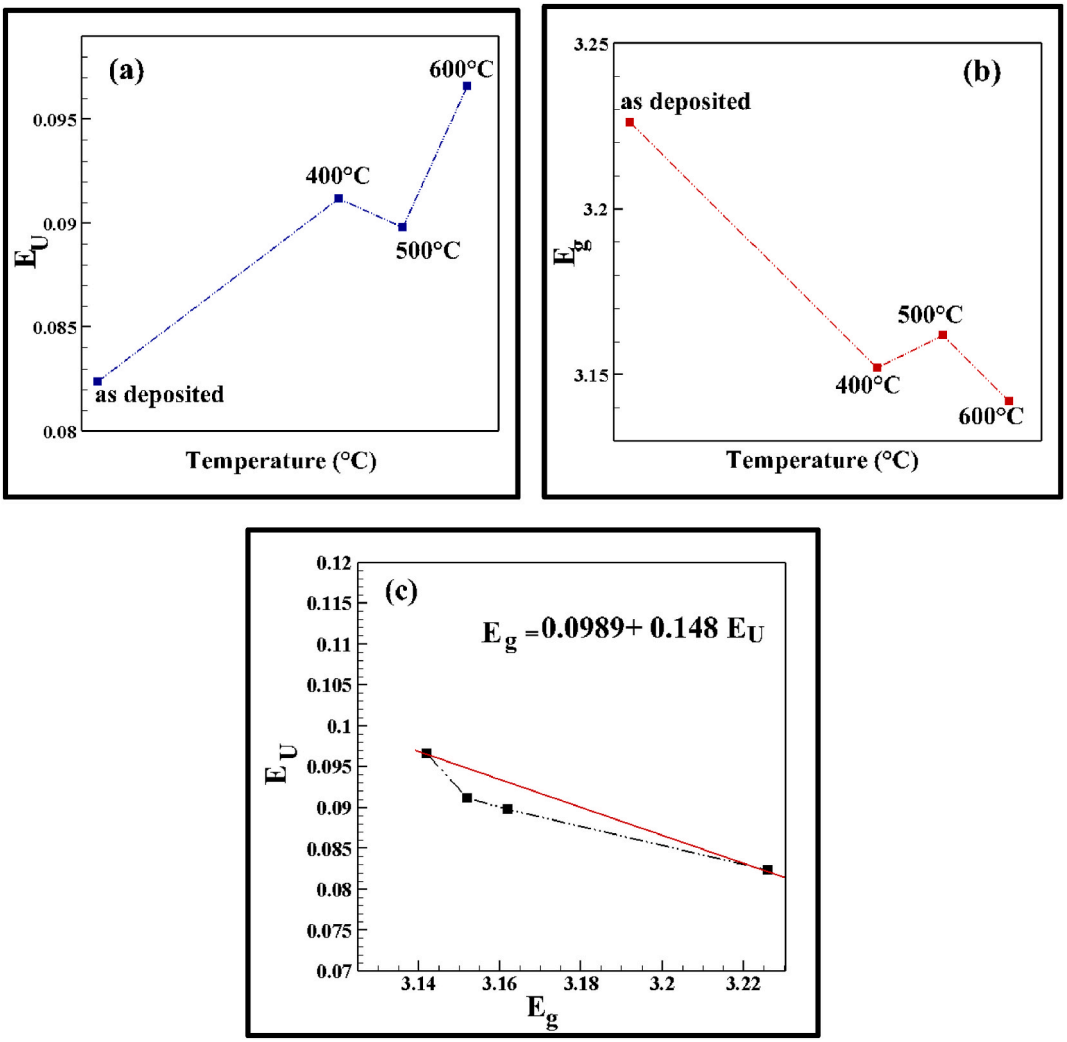

Fig. 9. (a) and (b) Temperature dependency of as deposited ZnO films and ZnO films annealed at 400, 500 and 600 °C on the optical energy gap and the band tail width, **(c)** and relation between the energy band gap and the width of the Urbach tails.

$\varepsilon_2\omega/4\pi$. The absorption coefficient of films can be used to calculate the optical conductivity σ_{opt} and electrical conductivity σ_{elec} as follows [37].

$$\boldsymbol{\sigma_{opt} = \varepsilon_2\omega/4\pi = \alpha nc \,/\, 4\pi\,\varepsilon_2 = 2nk;\ k = \varepsilon_0\alpha\lambda;\ \omega = 2\pi\, c/\lambda} \tag{13}$$

$$\boldsymbol{\sigma_{elec} = (2\lambda/\alpha)\sigma_{opt}} \tag{14}$$

Where α is the absorption coefficient of films and c is the light velocity (see Fig. 10). The variations of optical conductivity of as deposited ZnO films and ZnO films annealed at 400, 500 and 600 °C, versus photon energy were illustrated in Fig. 11 (a). Also, the

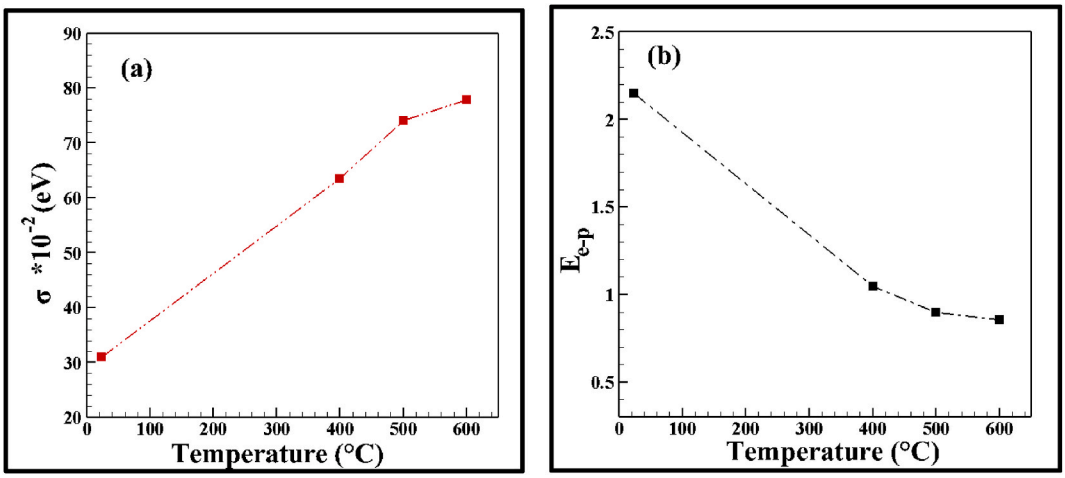

Fig. 10. The variations of both **(a)** the steepness parameters and **(b)** the electron-phonon interactions of as deposited ZnO films and ZnO films annealed at 400, 500 and 600 °C, versus annealing temperatures.

variations of electrical conductivity of as deposited ZnO films and ZnO films annealed at 400, 500 and 600 °C, versus photon energy were illustrated in Fig. 11 (b). The optical conductivity of films was increased with increasing in both photon energy and annealing temperature of the studied films and the electrical conductivities have the same behavior. The increasing in optical conductivity at high photon energies may be due to the high absorbance incident photons on surface these films [38].

3.4. Determination of the refractive index and film thickness

The obtained values of the refractive index *n* of films can be fitted based on the Wemple and DiDomenico model in the region from visible to near-infrared by the subsequent equation [21]:

$$(n^2\text{-}1)^{-1} = (E_0/E_d) - 1/(E_0E_d)(h\nu)^2 \quad (15)$$

Where E_o and E_d *and* $h\nu$ are the single-oscillator energy and dispersion energy parameter, the photon energy, respectively. The values of E_o and E_d were computed from the intercept E_o/E_d and the slope $E_oE_d^{-1}$ of the straight lines of the $(n^2\text{-}1)^{-1}$versus $(h\nu)^2$ relation as illustrated in Fig. 12 (a).

As mentioned, the values of E_o and E_d were to be found to have the same behavior. These values were large at 500 °C and 600 °C and have lower values at room temperature and 400 °C. The dispersion energy E_d obeys the following empirical relationship [39].

$$E_d = \beta N_c Z_a N e \quad (16)$$

where N_c is the coordination number of the cation nearest-neighbor to the anion, Z_a is the formal chemical valence of the anion, N_e is

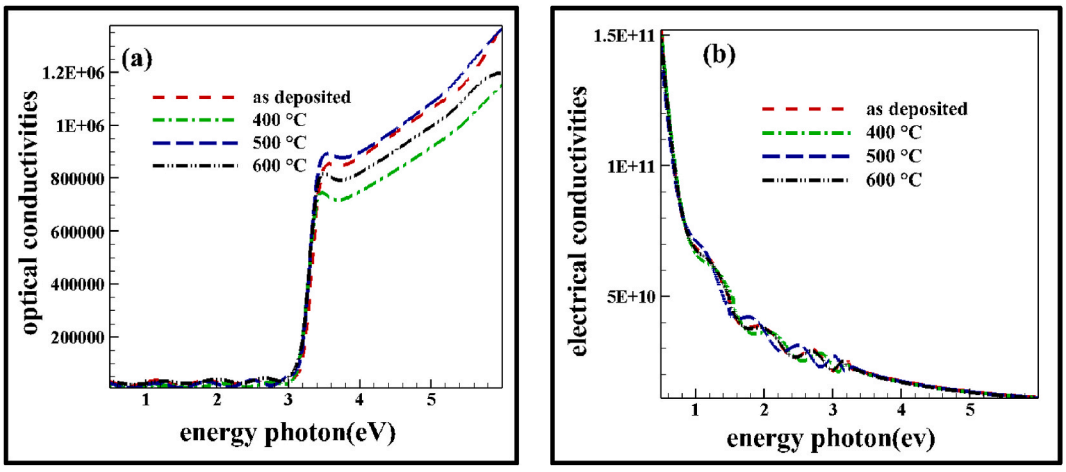

Fig. 11. The variations of (a) optical conductivity and (b) electrical conductivity of as deposited ZnO films and ZnO films annealed at 400, 500 and 600 °C, versus photon energy.

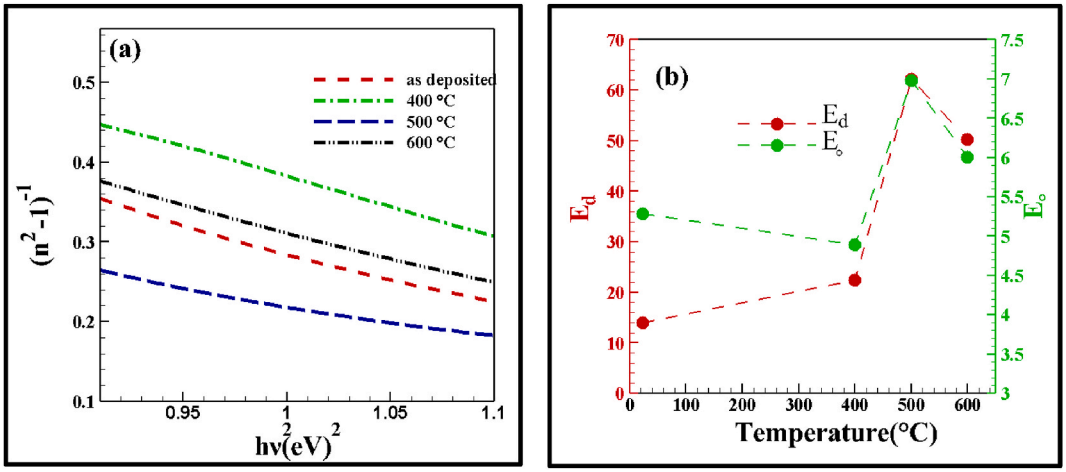

Fig. 12. (a) The variations of $(n^2-1)^{-1}$ of as deposited ZnO films and ZnO films annealed at 400, 500 and 600 °C, versus $(h\nu)^2$ and **(b)** the variations of both the E_o and E_d of as deposited ZnO films and ZnO films annealed at 400, 500 and 600 °C, versus the annealing temperatures.

the effective number of valence electrons per anion. This equation has an important constant parameter that is; β which it was to be indicated the ZnO films have to be type bonding and characterization. In these films due to condition imposed, for covalently bonded crystalline and amorphous chalcogenides the constant β has values of about 0.37 ± 0.04 and for halides and most oxides that have ionic structure the constant β has values of about 0.26 ± 0.04 eV. Taking $N_c = 4$, $Z_a = 2$, $N_e = 8$ for ZnO films [39], the values of β value for as deposited ZnO films and ZnO films annealed at 400, 500 and 600 °C, were determined and were reported in Table 2. As mentioned, the obtained values of β is in agreement with that published for ZnO films [39].

The variations of optical transmittance and reflectance spectra of films at different annealing temperature versus wavelength were shows in Fig. 13 (a).

The values of the refractive index n of these films must to be first be computed via the subsequent relation [40]:

$$\mathbf{S} = \boldsymbol{T_s^{-1}} + \left(\boldsymbol{T_s^{-1}} - \mathbf{1}\right)^{1/2} \tag{17}$$

The calculated crudes of refractive index n_1 for the as-prepared and annealed films under investigation can be computed based on envelope method via transmission spectrum proposed by Swanepoel [40,41]. The values of n_1 can be computed at any wavelength via the relation:

18.

Here T_M and T_m, are the value of transmission maximum and the value of corresponding minimum at a certain wavelength λ one of these values is an experimental interference extreme and the other one is derived from the corresponding envelope. The values of the refractive index n_1, were computed from equation (18), were shows in Table 3 and the values of n_1 at any adjacent maximal (or minimal), that have been computed by equation (18) and were used to deduce crude thickness of films, $d_{crude} = d_1$. If n_{e1} and n_{e2} to be the value of refractive indices of two adjacent maxima or minima at wavelengths λ_{e1} and λ_{e2}, then the crude thickness of as deposited ZnO films and ZnO films annealed at 400, 500 and 600 °C were expressed as [41]:

$$\mathbf{d} = \lambda_1\lambda_2 \,/\, \mathbf{2}(\lambda_1 \boldsymbol{n}_{\mathbf{e2}} - \lambda_2 \boldsymbol{n}_{\mathbf{e1}}) \tag{19}$$

The values of films thickness were listed in Table 3 and shown as d_1. To improve the accuracy of thickness of films there were a set of the order number m_o for the interference fringes which were resulted from relation [41]:

$$\boldsymbol{m_0} = \mathbf{2}\boldsymbol{n}_1\mathbf{d}_1/\lambda \tag{20}$$

In previous reports [42], the transmittance and reflectance spectra for films were showed. Next, by taking the approximate value of m_o, a new order number m is produced where $m = 1, 2, 3, \ldots$ at the maximum points in the optical transmission spectrum and $m = 1/2, 3/2, 5/2, \ldots$at minimum points in the optical transmission spectra. After that, the value of refractive index accuracy n_2 in terms of accuracy of thickness films, were expressed as d_2 which were obtained by the subsequent relation:

$$\boldsymbol{n_2} = \boldsymbol{m}\lambda/\mathbf{2}\mathbf{d_2} \tag{21}$$

Where d_2 is the new average accuracy of thickness of thin films after rounding m_o to m. The final values of new refractive index n_2 and other mentioned values are listed in Table 3. Then, for calculation of the standard deviation's values σ_i and deviation ratio p_i about the actual values for each which of d_1 and d_2, we use the subsequent relations [41]:

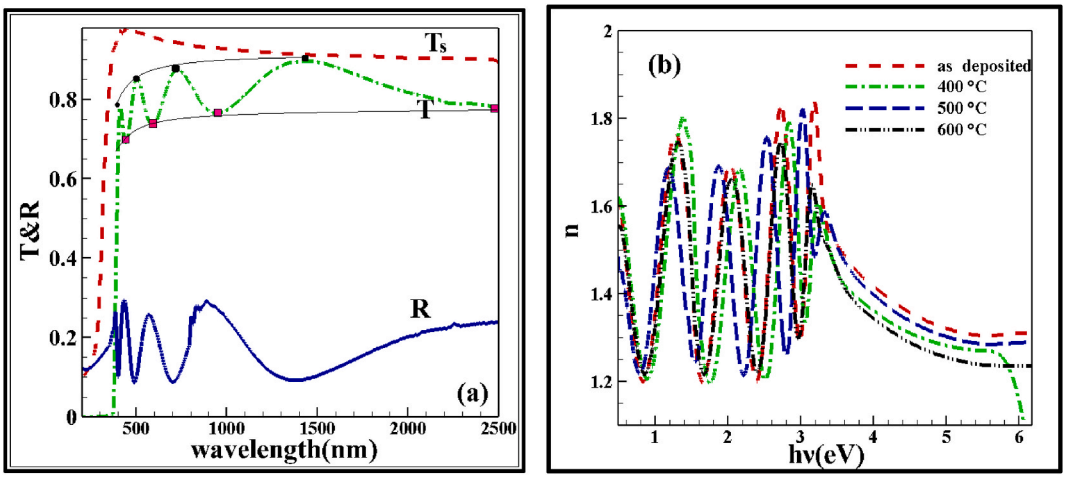

Fig. 13. (a) Variations of spectra transmittances and spectra reflectance of as deposited ZnO films and ZnO films annealed at 400, 500 and 600 °C, versus wavelength and **(b)** variations of values *n* of these films versus photon energy.

Table 3
Values of envelopes T_M and T_m of as deposited ZnO films and ZnO films annealed at 400, 500 and 600 °C, and the computed values of refractive index and films thicknesses are based on the envelope method.

Sample no.		λ	TM	Tm	Ts	S	n1	n2	d1(nm)	m0	m	d2(nm)	n
ad deposited ZnO films													
d1 = 510.47	σ1 = 1.83 %	446.95	0.85	0.72	0.97	1.21	1.94	1.93	696.25	6.04	1.66	191.8	1.75
d2 = 518.81	σ2 = 0.88 %	570.63	0.86	0.74	0.96	1.24	1.9	1.9	400	2.66	3.75	563.9	1.68
		840.08	0.87	0.74	0.93	1.36	1.97	1.9	519.38	2.43	3.25	692.9	1.82
		1674.9	0.88	0.79	0.91	1.23	1.83	1.83	426.24	1	1.37	626.8	1.84
ZnO films annealed at 400 °C													
d1 = 429.26	σ1 = 0.79 %	410.07	0.77	0.69	0.97	1.21	1.85	1.81	378.24	3.41	1.85	200.3	1.61
d2 = 517.88	σ2 = 0.95 %	502.02	0.85	0.71	0.96	1.24	1.98	1.96	429.17	3.39	2.37	599.7	1.79
		706.54	0.87	0.76	0.94	1.31	1.96	2.96	533.63	3.57	4.73	643.3	1.68
		1439	0.89	0.77	0.91	1.44	1.81	1.58	375.99	0.95	1.81	628.2	1.8
ZnO films annealed at 500 °C													
d1 = 505.84	σ1 = 5.33 %	450.02	0.86	0.75	0.97	1.21	1.98	1.97	534	4.69	4.76	541.4	1.81
d2 = 676.09	σ2 = 4.05 %	568.76	0.89	0.78	0.96	1.24	1.59	1.58	469.75	2.62	3.91	700.8	1.75
		836.12	0.92	0.81	0.93	1.36	2.05	20.4	534.87	2.62	1.03	826.8	1.69
		1554	0.93	0.82	0.93	1.35	2.07	2.07	484.72	1.29	1.69	635.3	1.68
ZnO films annealed at 600 °C													
d1 = 508.53	σ1 = 1.96 %	427.51	0.67	0.61	0.96	1.61	2.36	2.35	594.88	6.57	2.32	210.5	1.68
d2 = 466.70	σ2 = 1.84 %	523.93	0.75	0.63	0.97	1.22	2.2	2.2	494.48	4.15	3.9	464.7	1.69
		760.61	0.76	0.67	0.94	1.3	2.1	2.1	528.58	2.92	3.17	573.8	1.38
		1461.9	0.79	0.67	0.91	1.42	2.38	2.38	415.44	1.35	20.1	617.7	1.35

$$\boldsymbol{\sigma_i} = \left[\mathbf{1/n}\sum_{1}^{n}\boldsymbol{d_i^2} - \overline{\boldsymbol{d_i}}^{\mathbf{2}}\right]^{1/2};\ \overline{\boldsymbol{d_i}} = \mathbf{1}/\mathbf{n}\sum_{1}^{n}\boldsymbol{d_i};\ \mathbf{p_i}[\%] = \boldsymbol{\sigma_i}/\boldsymbol{d_i} \tag{22}$$

where *i* index is a number equal to 1 or 2 and *n* to be refers to the number of thicknesses. The accuracy of *d* can now be significantly were increased by considering the corresponding exact integer or half integer values of *m* associated with each extreme the optical transmittance and reflectance spectra and deriving a new thickness, d_2 relation (22). With using the values of n_1, the values of d_2 found in this way have a smaller dispersion ($\sigma_1 > \sigma_2$). It should be highlighted that the accuracy of the final thickness which approximately was better than 1 % (listed in Table 3). As shown in Table 3, with using the values of n_1, the values of d_2 found in this way have a smaller dispersion ($\sigma_1 > \sigma_2$). The accurate value of *n* in relationship (22) are obtained as listed in Table .3 can be solved by the exact value of m at each λ and, thus, the final values of the refractive index n_2. Fig. 12(b) shows the dependence of *n* films on photon energy. The refractive indexes of the films show that there was a normal dispersion in the spectral range of 0.5/hν (*eV*)/4.5 and an anomalous dispersion in *IR* range. The variations of the refractive index and extinction coefficients of films can be attributed to the optical absorption spectra, various of impurities and imperfection in films. Therefore, it can be expected that the structural disorders and defects in these films were occurred by changing the annealing temperature. The values of *n* can be fitted to a reasonable dispersion function which can be used for extrapolation the whole wavelength dependence of refractive index Fig. 13 (b).

4. Conclusions

The ZnO thin films deposited in room temperature on glass substrates by VAS- system rf magnetron system and ZnO composite target (100 mm diameter and 5 mm thickness with high purity (99.99 %)) and with a 13.56 MHz power supply, and also the reactor consisted of two electrodes with different sizes. Then these films were annealed at different annealing temperatures of 400, 500, and 600 °C in electrical furnace with Ar flux for 60 min.

It was found that:

1 With increasing annealing temperature, the values of nano particles size of films surface were increased from 20 to 30 nm, due to the increasing energy and surface mobility nano particles.
2 The RMS roughness of films annealed at 500 °C have minimum value in about 7 nm which in fact, 500 °C in an argon medium was a critical temperature for oxidative structure changes.
3 The coordination number β has a maximum value of 0.97 for ZnO thin films annealed at 500 °C.
4 The electron-phonon interaction of ZnO thin films annealed at 600 °C has a minimum value of about 0.85 eV.
5 The steepness parameters of ZnO thin films annealed at 600 °C have a maximum value of about 77.85 eV.
6 The empirical equations from linear fitting ln(α) of as deposited ZnO thin films has a maximum value of slop graph in about 12.13.
7 The empirical equation from these linear fitting for all ZnO thin films was given as $E_g = 0.0989–0.148\ E_U$.
8 The refractive index of ZnO thin films annealed at 500 °C has a maximum value of 1.81 in all energy ranges.
9 The value of E_0 and E_d in the ZnO thin films annealed at 500 °C have maximum values in about 7 and 65 eV, respectively.

Funding

There is not funding.

The data availability statement

The data that support the findings of this study are available from the corresponding author upon reasonable request.

CRediT authorship contribution statement

Vali Dalouji: Writing – review & editing, Writing – original draft, Visualization, Funding acquisition, Formal analysis.

Declaration of competing interest

The authors have no conflicts of interest to declare. All co-authors have seen and agree with the contents of the manuscript and there is no financial interest to report. We certify that the submission is original work and is not under review at any other publication.

Acknowledgements

Not applicable.

References

[1] D. Cotter, R.J. Manning, K.J. Blow, A.D. Ellis, A.E. Kelly, D. Nesset, I.D. Philips, A.J. Poustie, D.C. Rogers, Science 286 (1999) 1523.
[2] M. Lamrani, M. Addou, Z. Sofiani, B. Sahraoui, J. Ebothe, A.E.L. Hichou, N. Fellahi, J.C. Bernède, R. Dounia, Opt Commun. 277 (2007) 197.
[3] Z. Sofiani, B. Sahraoui, M. Addou, R. Adhiri, M. Alauoui Lamrani, L. Dghoughi, N. Fellahi, B. Derkowska, W. Bala, J. Appl. Phys. 101 (2007) 063104.
[4] K.P. Ghoderao, S.N. Jamble, R.B. Kale, Influence of pH on hydrothermally derived ZnO nanostructures, Optika - Int. J. Light Electron Opt. 156 (2018) 758–771.
[5] J. Singh, S. Kumar, Rishikesh, A.K. Manna, R.K. Soni, Optical Materials, Fabrication of ZnO–TiO2 nanohybrids for rapid sunlight driven photodegradation of textile dyes and antibiotic residue molecules, Opt. Mater. 107 (2020) 110138, https://doi.org/10.1016/j.optmat.2020.110138.
[6] J. Singh, R. Soni, Fabrication of hydroxyl group-enriched mixed-phase TiO_2 nanoflowers consisting of nanoflakes for efficient photocatalytic activity, J. Mater. Sci. Mater. Electron. 31 (2020) 12546–12560, https://doi.org/10.1007/s10854-020-03805-w.
[7] J. Singh, A. Manna, R. Soni, Bifunctional Au–TiO2 thin films with enhanced photocatalytic activity and SERS based multiplexed detection of organic pollutant, J. Mater. Sci. Mater. Electron. 30 (2019) 16478–16493, https://doi.org/10.1007/s10854-019-02023-3.
[8] J. Singh, R.K. Soni, Controlled synthesis of CuO decorated defect enriched ZnO nanoflakes for improved sunlight-induced photocatalytic degradation of organic pollutants, Appl. Surf. Sci. 521 (2020) 146420, https://doi.org/10.1016/j.apsusc.2020.146420.
[9] J. Singh, R.K. Soni, Efficient charge separation in Ag nanoparticles functionalized ZnO nanoflakes/CuO nanoflowers hybrids for improved photocatalytic and SERS activity, Colloids Surf. A Physicochem. Eng. Asp. 626 (2021) 127005, https://doi.org/10.1016/j.colsurfa.2021.127005.
[10] J. Singh, R.K. Soni, Tunable optical properties of Au nanoparticles encapsulated TiO2 spheres and their improved sunlight mediated photocatalytic activity, Colloids Surf. A Physicochem. Eng. Asp. 612 (2021) 126011, https://doi.org/10.1016/j.colsurfa.2020.126011.
[11] J. Labis, M. Hezam, A. Al-Anazi, H. Al-Brithen, A.A. Ansari, A.M. El-Toni, R. Enriquez, G. Jacopin, M. Alhoshan, Pulsed laser deposition growth of 3D ZnO nanowall network in nest-like structures by two-step approach, Sol. Energy Mater. Sol. Cells 143 (2015) 539–545.
[12] M. Opel, S. Geprägs, M. Althammer, T. Brenninger, R. Gross, Laser molecular beam epitaxy of ZnO thin films and heterostructures, J. Phys. D Appl. Phys. 47 (2013) 34002.
[13] M. Ortega-López, A. Morales-Acevedo, Properties of ZnO thin films for solar Cells grown by chemical bath deposition, in: Proceedings of the Conference Record of the Twenty Sixth IEEE Photovoltaic Specialists Conference, Anaheim, CA, USA, 1997, pp. 555–558.

[14] B. Wu, S. Zhuang, C. Chi, Z. Shi, J.Y. Jiang, X. Dong, W.C. Li, Y. Zhang, B.L. Zhang, G.T. Du, The growth of ZnO on stainless steel foils by MOCVD and its application in light emitting devices, Phys. Chem. Chem. Phys. 18 (2016) 5614–5621.
[15] L. Dejam, S.M. Elahi, H.H. Nazari, H. Elahi, S. Solaymani, A. Ghaderi, Structural and optical characterization of ZnO and AZO thin films: the influence of post-annealing, J. Mater. Sci. Mater. Electron. 27 (2016) 685–696.
[16] N. Rahimi, V. Dalouji, Study of the surface topography and optical properties of ZnO and AZO, CZO, and CAZO thin films (in room temperature and annealed at 500 °C), Mol. Cryst. Liq. Cryst. 753 (1) (2023) 73–87.
[17] A. Roudbari, V. Dalouji, S. Solaymani, N. Beryani Nezafat, S. Rezaee, The Effect of Geometry Characterizations and Annealing Processing on Dissipation Electrical Energy in ZnO Films, 2019, p. 40, article number 75.
[18] A. Liu, J. Zhang, Q. Wang, Structural and optical properties of zno thin films prepared by different sol-gel processes, Chem. Eng. Commun. 198 (2010) 494–503.
[19] J.F. Lei, Z.W. Wang, W.S. Li, Controlled fabrication of ordered structure-based ZnO fi lms by electrochemical deposition, Mater. Sci. Semicond. Process. 573 (2014) 74–78.
[20] B.M. Tienes, R.J. Perkins, R.K. Shoemaker, G. Dukovic, Layered phosphonates incolloidal synthesis of anisotropic ZnO nanocrystals, Chem. Mater. 25 (2013) 4321–4329.
[21] N. Rahimi, V. Dalouji, S. Rezaee, Effect of annealing processing on morphology, spectroscopy studies, Urbach disordering energy, and WDD dispersion parameters in Cu-Al doped zinc oxide films, J. Dispersion Sci. Technol. (2020).
[22] L. Irimpan, D. Ambika, V. Kumar, V.P.N. Nampoori, P. Radhakrishnan, Effect of annealing on the spectral and nonlinear optical characteristics of thin films of nano-ZnO, J. Appl. Phys. 104 (2008) 033118.
[23] N. Rahimi, V. Dalouji, A. Souri, Studying the optical density, topography, and structural properties of CZO and CAZO thin films at different annealing temperatures 6 (No.2) (2020) 17–23.
[24] A.S. Hassanien, A.A. Akl, Influence of composition on optical and dispersion parameters of thermally evaporated non-crystalline Cd50S50-xSex thin films, J. Alloys Compd. 648 (2015) 280–290.
[25] S.S. Chiad, Optical characterization of NiO doped Fe2O3 thin films prepared by spray pyrolysis method, Int. Lett. Chem. Phys. Astron. 6 (2015) 50–58.
[26] J.F. Eloy, Power Lasers. National School of Physics, Wiley, Grenoble, France, 1984.
[27] P. Abbasi, V. Dalouji, Influence of Annealing Processing on Dissipation Electrical Energy, Volume, and Surface Energy Loss Functions of CZO Films, Indian J Phys, 2020.
[28] J.D. Dow, D. Redfield, Phys. Rev. B 5 (1972) 594.
[29] G.D. Cody, T. Tiedje, B. Abeles, B. Brooks, Y. Goldstein, Phys. Rev. Lett. 47 (1981) 1480.
[30] S.M. Wasim, G. Marin, C. Rincon, G.S. Perez, J. Appl. Phys. 84 (1998) 5823.
[31] S. Goudarzi, V. Dalouji, The effect of Cu content in MWCNTs synthesized by Ni - Cu @ a-C: H catalyst on the optical constants and the optical loss, Optik 223 (2020) 165585.
[32] S. Goudarzi, V. Dalouji, S. Solaymani, The Relation between the Average Diameter of CNTs on Ni-Cu @ A-C:H Catalyst with the Optical Absorption Edge and the Optical Dispersion Parameters, 2020.
[33] S.J.I. khmayies, R.N. Ahmad-Bitar, A study of the optical bandgap energy and Urbach tail of spray-deposited CdS: in thin films, Mater. Res. Technol. 2 (2013) 221–227.
[34] K.N. Tonny, R. Rafique, A. Sharmin, et al., Electrical, optical and structural properties of transparent conducting Al doped ZnO (AZO) deposited by sol-gel spin coatin, AIP Adv. (2018).
[35] S. Wu, S. Yuan, L. Shi, et al., Preparation, characterization and electrical properties of fluorine-doped tin dioxide nanocrystals, Colloid Interface Sci. 346 (2010) 12–16.
[36] M.S. Bashar, M. Rummana, S. Munira, S. Ayesha, M. Rahaman, M.A. Gafur, F. Ahmed, Effect of rapid thermal annealing on structural and optical properties of ZnS thin films fabricated by RF magnetron sputtering technique, Theoretical and Applied Physics (2019).
[37] J.I. Pankove, Optical Processes in Semiconductors, Courier Corporation, New York, 1975.
[38] F. Yakuphanoglu, A. Cukurovali, I. Yilmaz, Opt. Mater. 27 (2005) 1363.
[39] S.H. Wemple, M. DiDomenico, Optical dispersion and the structure of Solids, Phys. 23 (1969) 1156.
[40] F.A. Jenkins, H.E. White, Fundamentals of Optics, McGraw-Hill, NewYork, 1957.
[41] J.C. Manifacier, J. Gasiot, J.P. Fillard, A simple method for the determination of the optical constants n, k and the thickness of a weakly absorbing thin film, PhysicsE: Scientific Instruments 9 (11) (1976) 1002.
[42] A. Roudbari, V. Dalouji, S. Solaymani, N. Beryani Nezafat, S. Rezaee, The effect of geometry characterizations and AnnealingProcessing on dissipation electrical energy in ZnO films, Int. J. Thermophys. (2019).